GBT Commissioning Memo: 25

GBT Calibration and Efficiency at 285-400 MHz

July 13, 2004

Glen Langston and Chris Orban

Number 1.0

Abstract

Calibration data for the GBT 285 to 400 MHz feed is presented, based on observations of bright radio source 3C295. We show good performance over the frequency range, but further confirming observations are required. The measured efficiency is slightly higher than expected, for the low frequency end of the band, but the source model and calibration noise diode values may contribute to the measurement. The average efficiency over the frequency 285 to 400 MHz is 73 ±9 %.

These observations should be repeated for other reference sources, in order to distinguish between source model errors and noise diode value uncertainty. These observations were made with the receiver with the Circular Polarization electronics activated. These observations should also be repeated in Linear polarization mode, where the noise diode values are better determined.

An appendix summarizes the AIPS++ functions used to generate these spectra and also shows the spectra of radio source 3C48. The 3C48 spectra are significantly worse due to radio frequency interference (RFI).

1 Introduction

These observations were made to calibrate data from a search for flaring emission from extra-solar planets. Because these observations are among the first performed in spectral line mode in this frequency band with the GBT, the calibration process is described in some detail.

These observations were performed in using the GBT Observe (GO) user interface procedure OFFON, which makes equal duration observations at a nearby location Off the source and on the source.

Below, the observing setup is presented, followed by a scan summary. The steps in calibrating the data are shown in some detail.

Section 2 describes the observing setup. Section 3 describes the process of calibrating the observations, including correcting for the system temperature variations across the observing band. Section 4 summarizes the short intensity variations and the possible effects on observation of radio flare events. Section 5 discusses the limitations on measurement of GBT efficiency in this frequency range. Appendix A describes the AIPS++ glish scripts used to generate the figures in this document.

Figure 1 shows a summary of the measurements of GBT efficiency in the frequency range 285 to 400 MHz. The figures shows 3 pairs of spectra obtained in 3 pairs of OFFON observations. The spectra and efficiency measurements were independently calibrated and the good efficiency agreement between the separate observations is encouraging.

The remainder of this document describes the steps performed to obtain the efficiency versus frequency plot.

2 Observing Setup

The data presented here were made on 2002 August 28 to calibrate the flare star search data obtained by Langston, Bastian and Orban. These observations were made with the GBT and PF1 receiver in good weather. The PF1 receiver had the 342.5 MHz feed installed and was configured for circular polarization observations.

The GBT RF/IF electronics was set up with glish script `/home/gbtops/include/rfi_300.g`. The first LO was configured for topocentric (fixed) frequency observation. IF rack modules 5 and 7 were connected to converter rack modules 9 and 13. The converter rack outputs were configured for input to analog filter rack modules 9 and 13, with the 50 MHz IF filter selected.

The spectrometer was the used, with the dual polarization, 9 level, 50 MHz, signal quadrant configuration selected. The autocorrelations had 8192 lags. The spectrometer controlled the noise diode cal on/off and blanking signals. LO blanking was not selected. The spectrometer was configured for 1 second integrations, and the scan durations were 30 seconds for these tests.

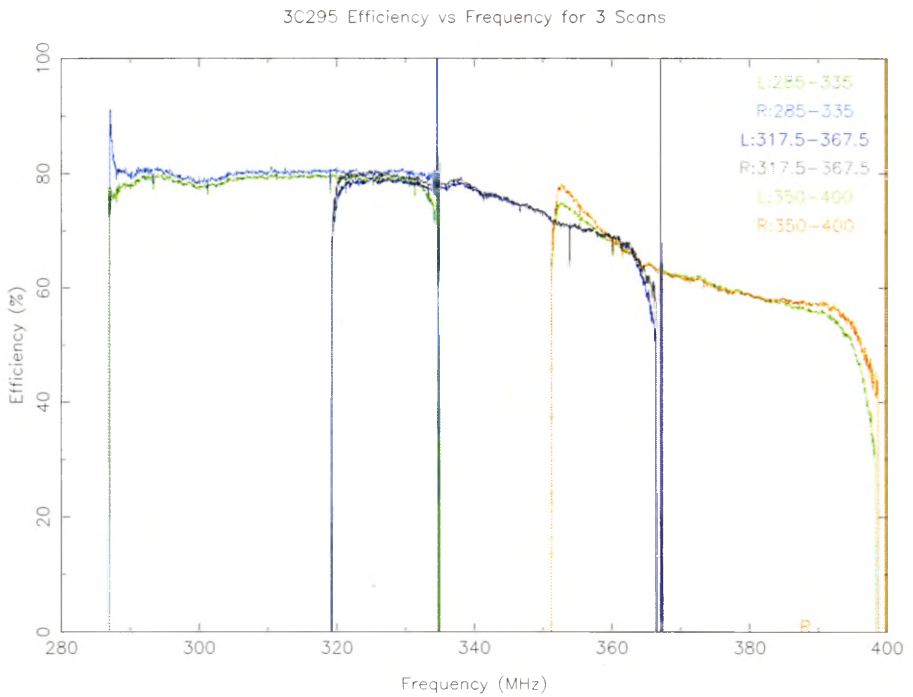

Figure 1: Measured GBT 285-400 MHz efficiency based on observations of 3C295 over 3 spectral ranges in 3 OFFON scan pairs. The observations were made in independent OFFON scan pairs. The efficiency measurements at the edges of the spectral windows are uncertain. Note the good agreement in the frequency ranges where the spectra overlap.

Name	Center Frequency (MHz)	Observing Duration (s)	Start Time	Start Scan	Stop
3C48	327	62	2002/08/28 02:59:31	836	837
3C295	310	62	2002/08/28 23:43:29	8	9
3C295	342.5	62	2002/08/28 23:49:37	10	11
3C295	342.5	62	2002/08/28 23:51:34	12	13
3C295	375	62	2002/08/29 00:01:51	14	15
3C295	375	62	2002/08/29 00:04:20	16	17
3C295	310	62	2002/08/29 00:09:03	18	19

Table 1: Observing log for calibration observations of 2002 August 28-29.

3 Calibration

The two polarizations of spectral data were separately calibrated in a series of steps, described below:

Averaging The data were obtained in a series of OFFON scans. These raw data (counts) were averaged, keeping separate the Signal Scans and Reference Scans (figure 2).

T_{Source} The first step in examining the data was performed using an estimated system temperature value, T_{sys} = 70K, that was assumed to be constant across the band. This allows the entire off source spectrum to be used in the calibration process, and is less sensitive to RFI than directly using difference between Noise Cal On and Off measurements (figure 3).

$$T_{Source} = 70K \frac{Sig - Ref}{Ref}$$

$T_{sys,ref}$ **Calculation** All reference spectra were averaged, separating Cal noise diode On and Off data. After all data from all reference scans were averaged, the average and difference of the signal level with Cal On, C_{on} and Cal Off, C_{off}, were computed. The laboratory noise diode data were spline interpolated used to generate a T_{cal} spectrum.

$$T_{sys,ref}(\nu) = T_{cal}(\nu) \times \frac{C_{on,ref}(\nu) + C_{off,ref}(\nu)}{2(C_{on,ref}(\nu) - C_{off,ref}(\nu))}$$

T_{sys} **Fit** The reference $T_{sys,ref}$ spectra were fit with a second order polynomial which fit the data reasonably well over the frequency range.

T^*_{source} The fits to the reference source spectra ($T_{sys,ref}$) were multiplied to the source spectra. This yields source spectra corrected for system temperature changes across the band.

$$T^*_{source}(\nu) = \frac{T_{sys,ref}(\nu)}{70K} T_{source}(\nu)$$

Figures 4 and 5 show LCP and RCP reference spectra and second order polynomial fits.

Source Model Ott *et al.*1994, models for sources 3C295 and 3C48 flux densities were implemented in AIPS++. This function (in `ott.g`) was used to calculate the source intensities for all spectral channels.

Efficiency Data The ratio of the model source flux to observed T_{Source} is proportional to the efficiency of the GBT. Assuming a K/Jy = 2.846 K/Jy for a 100% efficient 100m telescope, the efficiency curves were calculated based on the observed temperature and model flux densities.

$$Efficiency \equiv \frac{T_{source}}{2.846 S_{source}}$$

Figure 6 shows the measured efficiencies for LCP and RCP.

Efficiency Fit The efficiency data show a number of spectral features that are more likely due to frequency structure of the source or RFI. These effects are reduced by fitting the efficiency data with a second order polynomial. The efficiency fit is used for correcting the GBT observations of the program sources. Figure 7 shows a second order fit to the measured efficiencies for LCP and RCP.

Figures 8 and 9 show the calibrated reference source spectra and the Ott *et al.*model. Note that this processing enforces agreement between the data to second order. However the relatively good agreement between LCP and RCP fits and the small frequency variations are encouraging.

4 Intensity Variations

The purpose of this calibration process was to detect variations towards extra-solar planets. Clearly the spectral variations towards the reference direction and the reference source set guidelines as to what level of spectral variation might be detectable by this type of observation.

Because there are frequency ranges where RFI is strong, weak spectral variations may only be detected in carefully selected frequency ranges.

Figure 9 shows the intensity versus integration in a narrow frequency band, 342.5 to 343.5 MHz, relatively free of RFI. Notice the stronger variations in intensity towards 3C295.

Figure 10 shows the same as figure 9, except the average intensity in the signal scan is subtracted, leaving only the time variable part of the 3C295 observation. Whether the variation is due to RFI or scintillation can not be confirmed by these tests. However RFI would not be expected to show similar behavior in both circular polarizations.

The Appendix shows similar figures for 3C48. For the 3C48 observations the agreement between LCP and RCP efficiencies is not as good as for 3C295. There seems to be a systematic difference between two polarizations for the reference position spectra for the 3C48 observation. Since the spectra are calibrated by division by the reference spectra, differences in the reference spectra result in differences efficiency measurements. However large differences in circular polarization intensity for the reference position spectra are not expected.

5 Discussion

These observations show that the 285-400 MHz frequency range is occasionally free of strong RFI, and that sensitive measurements of spectral intensity can be made, if the RFI can be avoided.

The GBT 285-400 MHz efficiency is measured by these observations towards 3C295. The measured efficiency is somewhat higher than expected in the 285 to 340 MHz range. The discrepancy between observed and measured values may be due to errors in the Ott *et al.*1994 model for 3C295, or in the laboratory measurement of the calibration noise diode values.

Note that the noise diode values used here are the average of the Linear X and Y polarization values. There are only small intensity differences between the X and Y values, and these were averaged to get the estimated LCP and RCP values. These observations should be repeated using X and Y linear as well as R and L circular polarization towards several reference sources.

References

Ott *et al.*(1994), *A&A*, **284**:331)

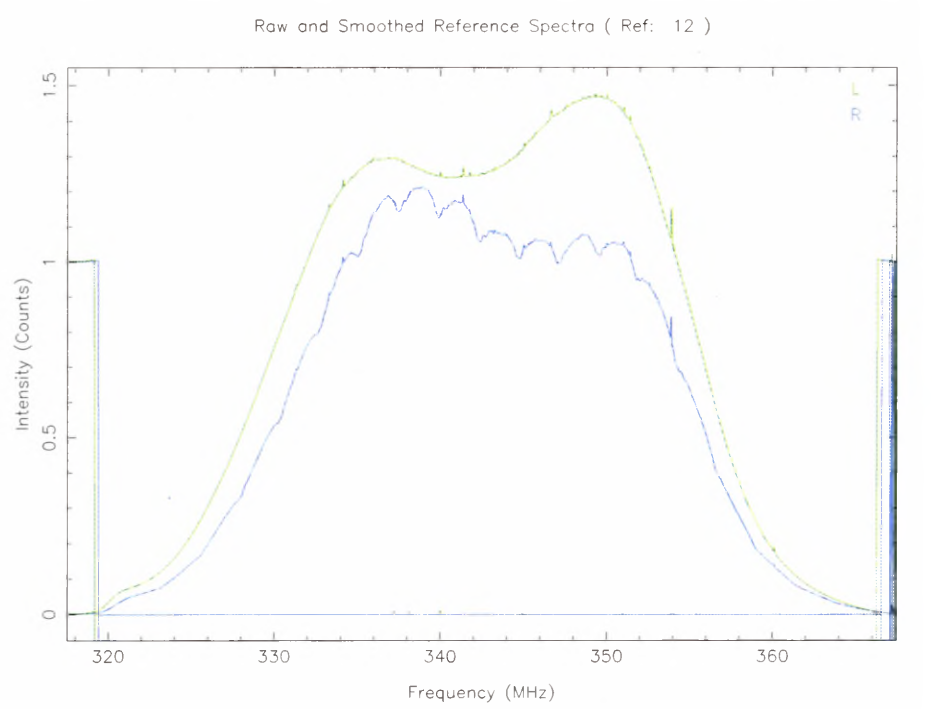

Figure 2: 3C295 raw reference spectra for LCP and RCP for the frequency range 317.5 to 367.5 MHz. These spectra show the effect of the 20 MHz receiver filter on the IF gain. The narrow receiver filter was selected to reduce out of band RFI. The IF rack gain ripple in module 7 is visible. The lower curves show the RFI detected in the reference spectra.

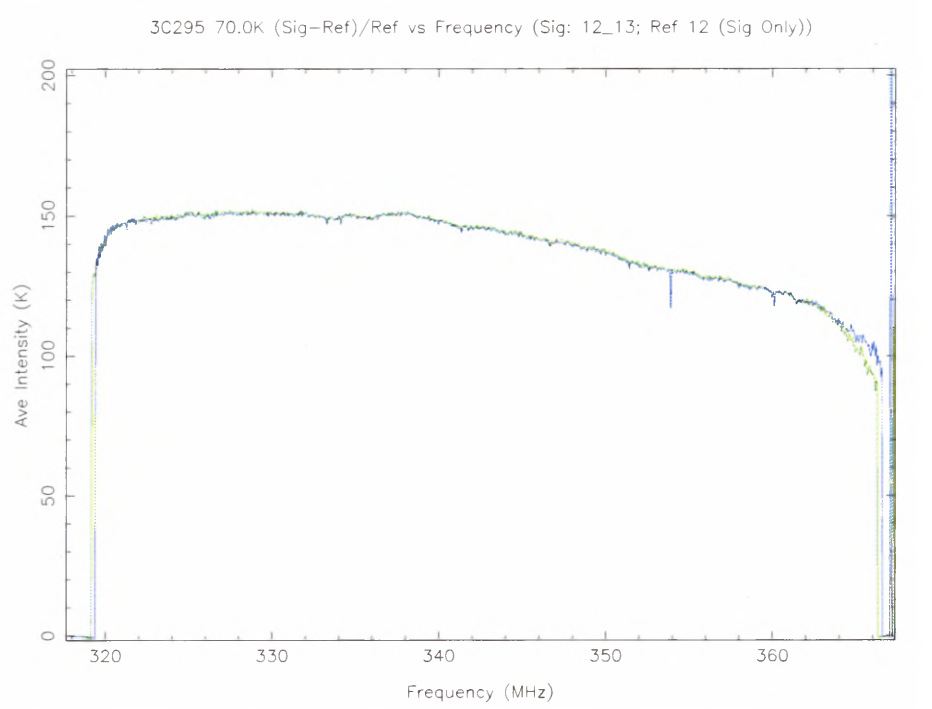

Figure 3: LCP and RCP spectra of 3C295 produced by $T_{sys}\times$ (Signal-Reference)/Reference calibration. This is the output of the `flare([12,13],[12])` glish script, were scans 12 and 13 were processed. The reference scan number is 12. Notice the IF gain ripple is successfully calibrated out.

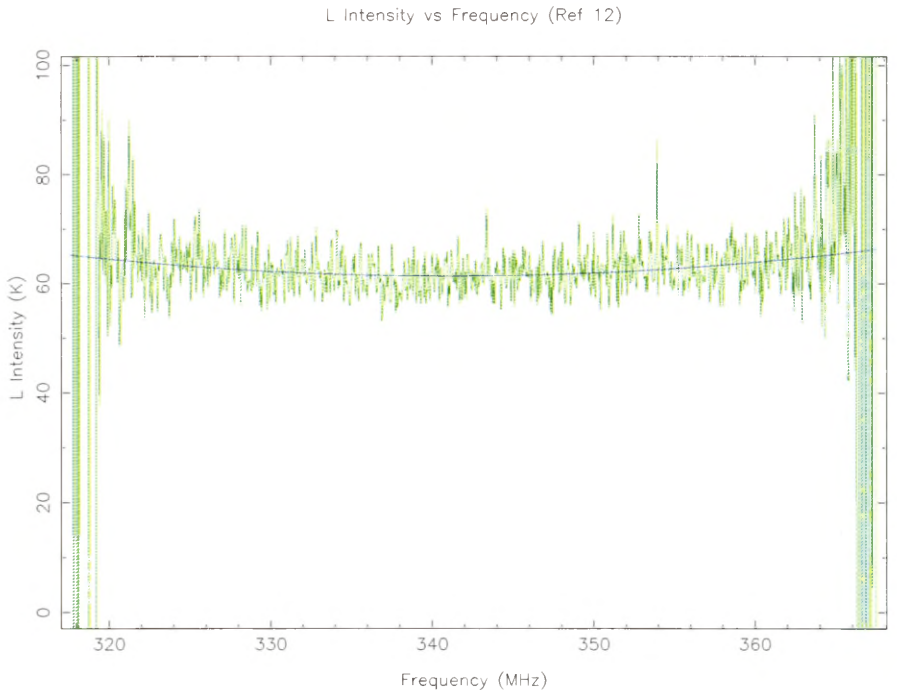

Figure 4: LCP spectrum measured for the system temperature of the reference scan, 12. A second order polynomial is fit to the data.

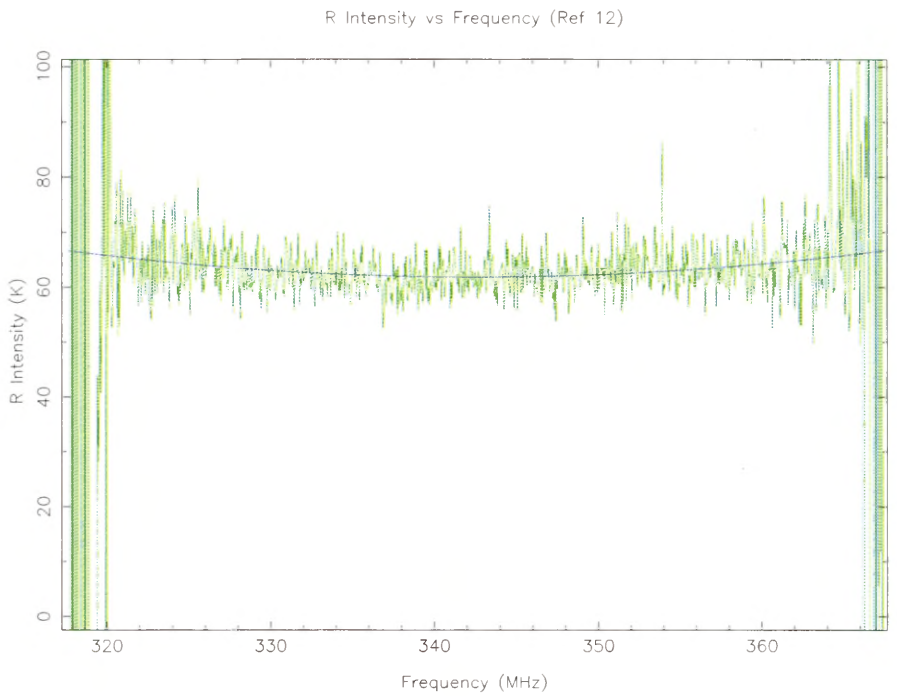

Figure 5: RCP spectrum measured for the system temperature of the reference scan, 12. A second order polynomial is fit to the data.

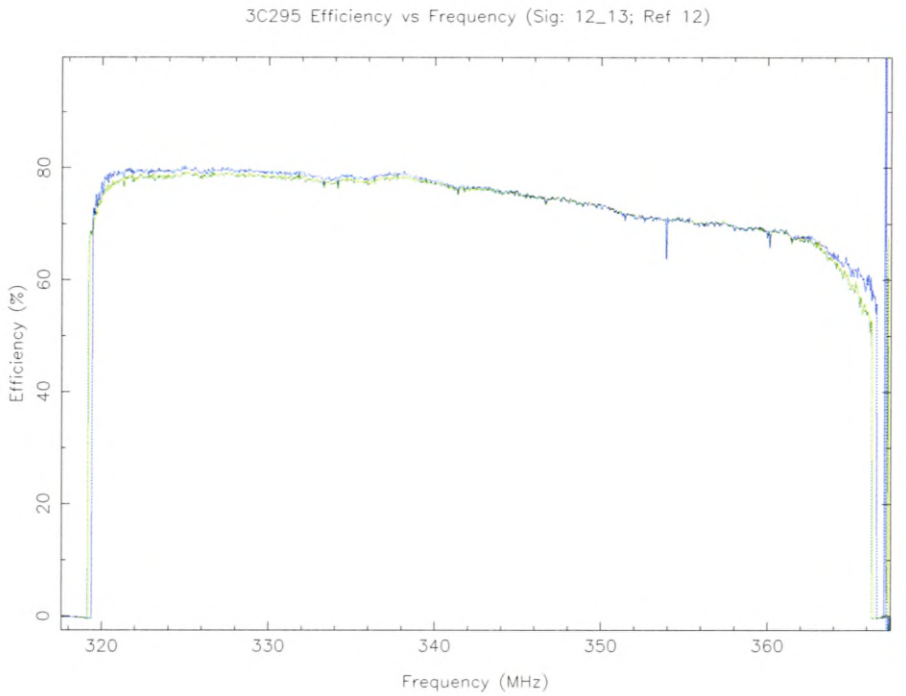

Figure 6: Measured GBT Efficiency based on observations of 3C295. This and the following plots are produced by glish scripts: `setFluxes(); updateEfficiency()`

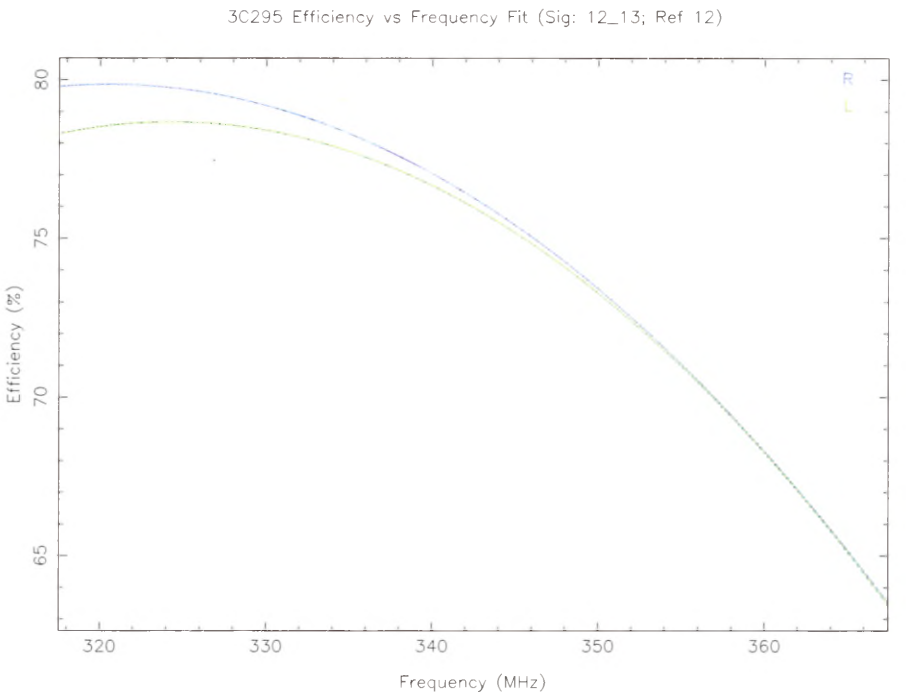

Figure 7: Fit to 3C295 LCP and RCP efficiency data, over the central 80% of the data in the previous plot.

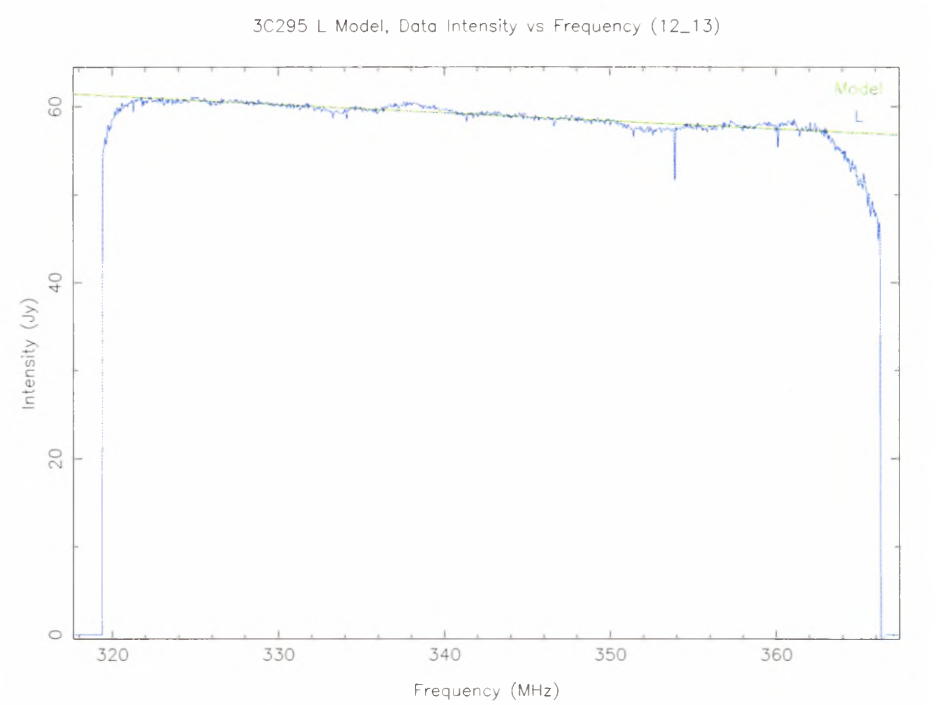

Figure 8: Spectral comparison of the calibrated 3C295 LCP observation with the Ott *et al.*1994 model for 3C295.

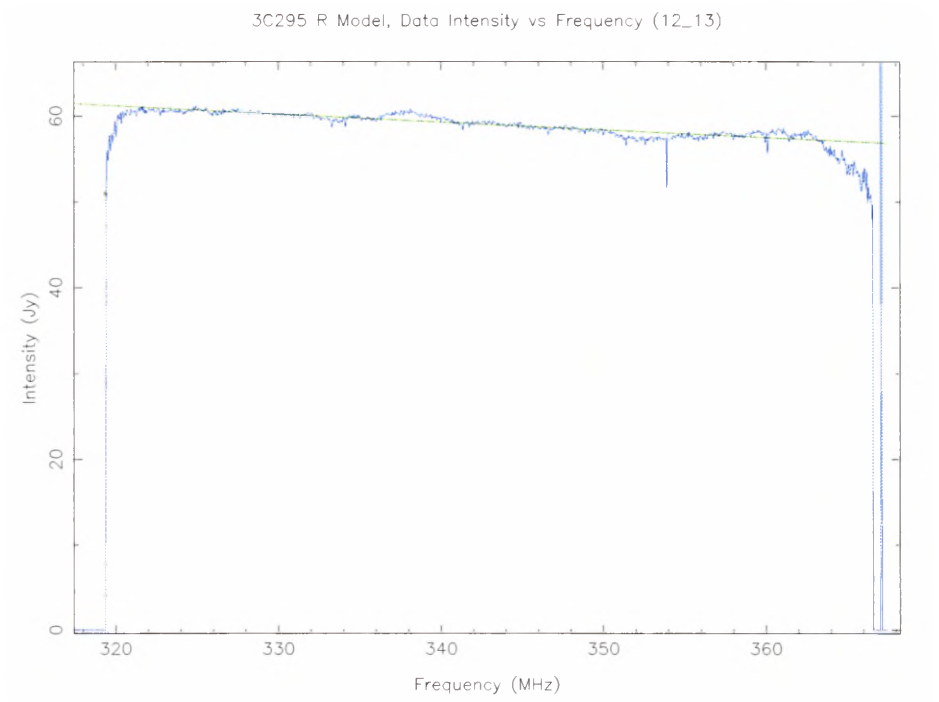

Figure 9: Spectral comparison of the calibrated 3C295 RCP observation with the Ott *et al.*1994 model for 3C295.

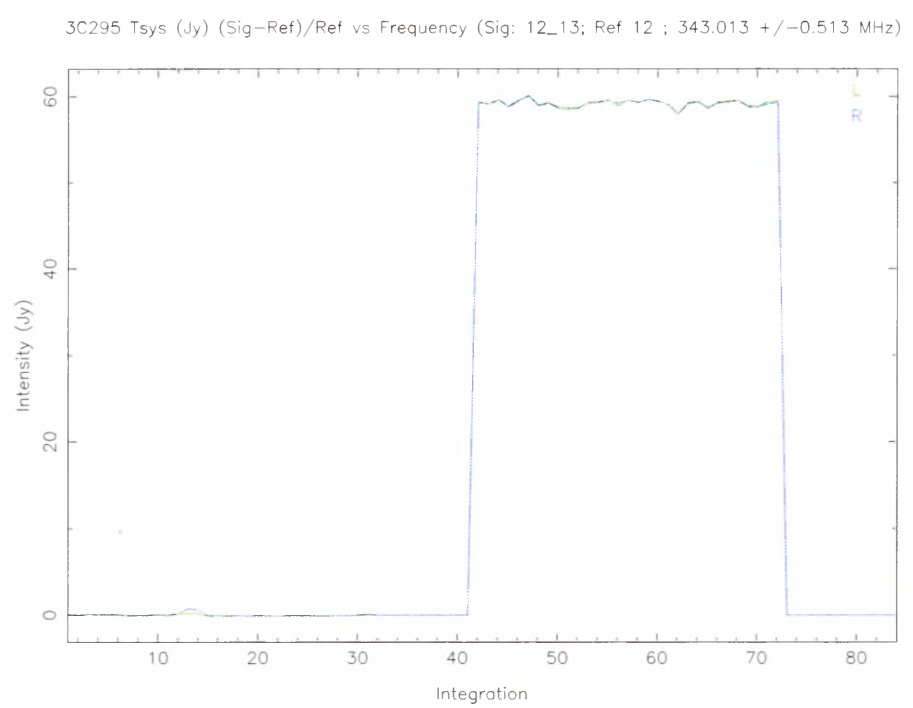

Figure 10: Average intensity versus time plot for the frequency range 342.5 to 343.5 MHz for reference and signal scans towards 3C295. The data are $T_{sys} \times (Sig - Ref)/Ref$ calibrated separately for LCP and RCP data. The average reference spectra for this time range was subtracted from both reference and signal. There are 10 integrations with zero intensity after each scan.

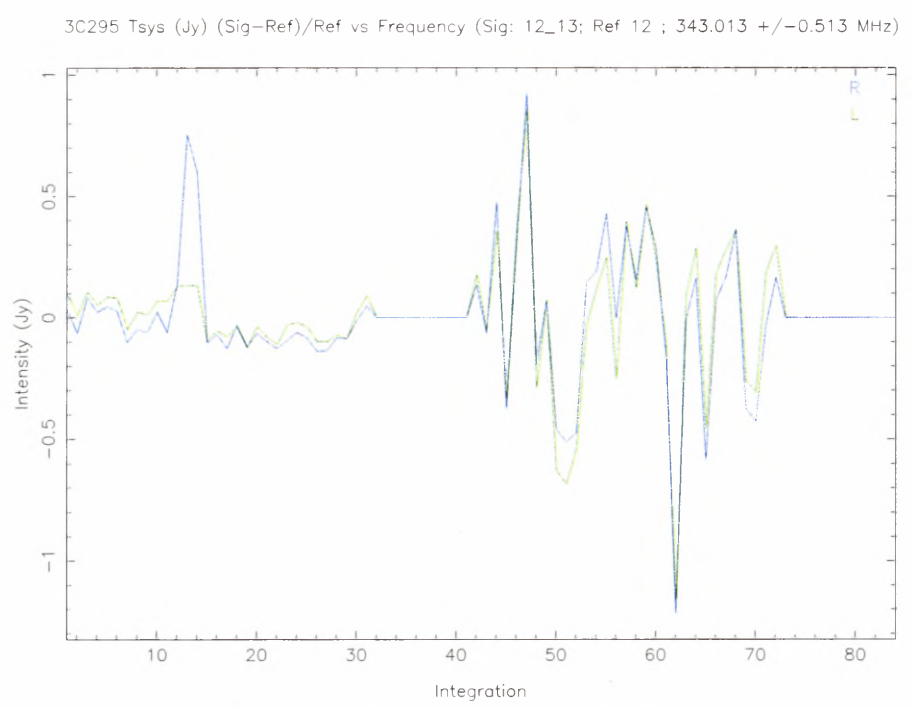

Figure 11: Average intensity versus time plot for the frequency range 342.5 to 343.5 MHz for reference and signal scans towards 3C295. The plot is the same as the previous plot, except that the average 3C295 intensity is subtracted from the signal scan. This shows the increased intensity variations toward 3C295.

Glish File	Function Name	Summary
flare.g	flare()	Reads a set of scans and produces average spectra
		Produces separate polarization images of all scans
flareRaw.g	flareRaw()	Reads all integrations of a single scan
flareSigRef.g	flareSigRef()	Keeps track of signal and reference scans
		Makes scan images, averages reference scans
flareCollage.g	flareCollage()	Combines scan images into a pair of images
	removeSignal()	Subtracts average signal spectra from images
flareCalib.g	updateEfficiency()	Calculates efficiency factors
	updateSigRefT()	Applies $T_{sys,ref}$ correction
	updateSigRefE()	Applies efficiency correction
flarePlot.g	pairPlot()	Plots intensity vs frequency
	efficiencyPlot()	Plots efficiency vs frequency
flareIntensity.g	intensityFreq()	Produces intensity versus integration plots
flareImage.g	flareImage()	Produces image from data arrays
ott.g	ottFlux()	Computes flux density for source, frequency
300MHzCal.g		Sets noise diode values for 300 MHz circular polarization

A Glish Scripts

The observations presented here were reduced using AIPS++ and glish scripts written by Chris Orban and Glen Langston in summer 2002. A short summary of these scripts is provided. These `flare.g` scripts are available within AIPS++ in Green Bank, upon request.

The scripts are intended for use in detecting time-frequency variations in spectra obtained with the GBT. At low frequencies and short integration times, the low calibration noise diode values are too faint for reliable intensity calibration. Alternatively the high calibration noise diode values could be used, or the spectral can be calibrated by averaging the reference spectra over number of scans. This approach was implemented in the `flare.g` scripts.

A sample AIPS++ execution is given below, assuming AIPS++ is started and the scripts are in the search path:

```
- include 'flare.g'

Plot functions for flare searches:
flarePlotRaw()     : Plots raw reference spectra
pairPlot(arrayX, arrayY, title, labelX, labelY,
         arrayXLabel, arrayYLabel): plots pair of arrays with titles
pairXYPlot( arrayX, arrayY, noteString): plot pair of Kelvin arrays
flarePlotDiff()    : Plots reference Cal On-Cal Off, X and Y arrays
sigRefPlot()       : XY plots average of all tSys*(Sig-Ref)/Ref

Calibration scenario:
flare()            : Create Sig-Ref Spectra for a calibration source
setFluxes()        : Set cal source flux model based on Ott etal 1994
updateEfficiency(): Update sigRef array for Tsys measurements
  the sigRef temps ARE updated for Tsys measurement, not efficiency
updateSigRefE()    : Update sigRef for efficiency measurements
modelDataXPlot()   : Check source data and model
collageInit()      : Zero sigRef, collage arrays, not efficiency
flare()            : Reduce program source data
flareTemps()       : Fit the program source Tsys measurements
updateSigRefE()    : Update program source data for efficiency
   using the calibraiton source efficiency fit

efficiencyPlot()   : Plots X,Y ratio of measured source to model flux
tSysPlot()         : plots the Calibrated X,Y Tsys data
tSysFitPlot()      : plots the Calibrated Fits to X,Y Tsys data
tSysXPlot()        : plots the Calibrated and Fit X Tsys data
```

```
tSysYPlot()       : plots the Calibrated and Fit Y Tsys data

Functions to search for Flaring events in a series of OFFON scans
flare(scanList, referenceList): processes a series of scans
flareWrite()     : Write a series of processed scans
flareRead()      : Restore a series of processed scans
removeSignal()   : Remove average signal spectra from source scansT
```

A help summary is printed after the scripts are loaded

```
- dopen( 'G01A54_01_SPECTROMETER_A')
T
-
- tSys :=  70.
- bandWidth := -50
- # line width for reject RFI before division by average reference
- referenceLineWidth := 7
- numchan := 8191
- refChan := (numchan+1)/2
-
- # set width for averaging channels
- averageWidth := 8
- include 'ott.g'                 #prepare to get the Ott et al fluxes
T
-
- include '300MHzCal.g'
T
- flare( [836,837], [836])        #process 2 scans [836, 837], reference is 836
...  Messages tracking script progress ...
T
- setFluxes()                     #calculate the flux for ''objectName''
Calculating Ott etal 1994 source fluxes for objectName: 3C48
This takes some time....
ottFlux: 3C48 [351.951172 351.902344 351.853516]  ... MHz
T
- updateEfficiency()              #calculate the efficiency factors
updateEfficiency: Setting tSys values with flareTemps()
...
T
- efficiencyPlot()                #show the efficiency plots
3C48 Efficiency vs Frequency Data (Sig: 836_837; Ref 836)
T
- updateSigRefE()                 #Modify spectra and miages
Scaling sigRefCalX,Y:= sigRefCalX,Y * efficiencyFactorX,Y
Scaling collage arrays: 84 Integrations
T
- modelDataXPlot()                #compare model and data, first pol
T
- modelDataYPlot()                #compare model and data, second pol
T
- intensityFreq( 342.5, 343.5)    #plot intensity versus time
...
Scan  836: Mean   0.000+/-  0.071 Jy    0.000+/-  0.047  343.016 (31)
Scan  837: Mean  44.760+/-  1.633 Jy   44.836+/-  1.544  343.016 (31)
T
- removeSignal()                  #remove average signal from all spectra
Finding Sig,Ref in Collages: 1023 84
...
T
- intensityFreq( 342.5, 343.5)    #plot intensity versus time again
...
Scan  836: Mean   0.000+/-  0.071 Jy    0.000+/-  0.047  343.016 (31)
Scan  837: Mean   0.000+/-  1.633 Jy    0.000+/-  1.544  343.016 (31)
```

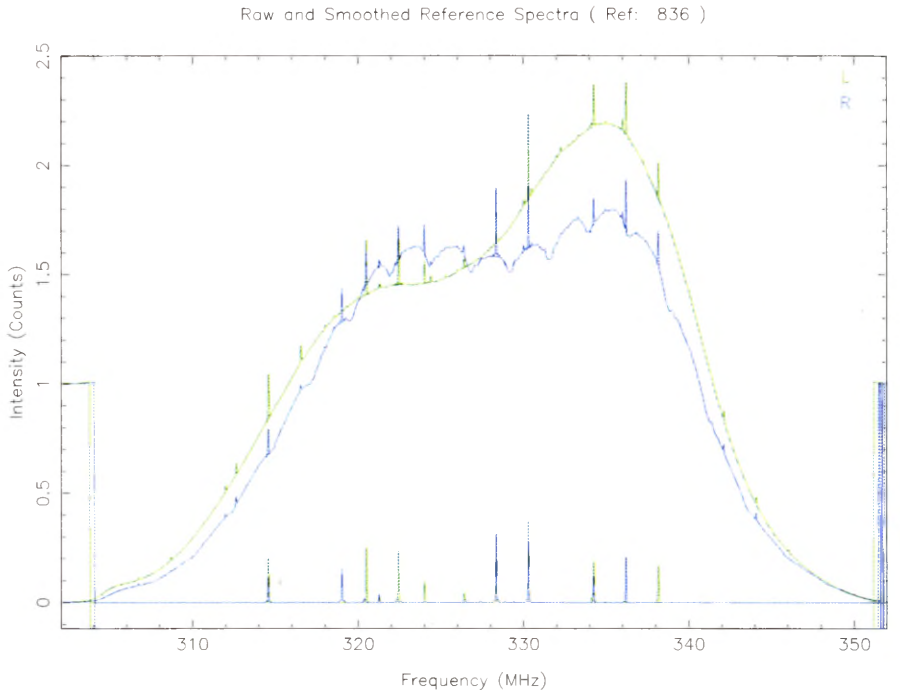

Figure 12: 3C48 raw reference spectra for LCP and RCP for the frequency range 302 to 352 MHz. The lower curves show the RFI detected in the reference spectra.

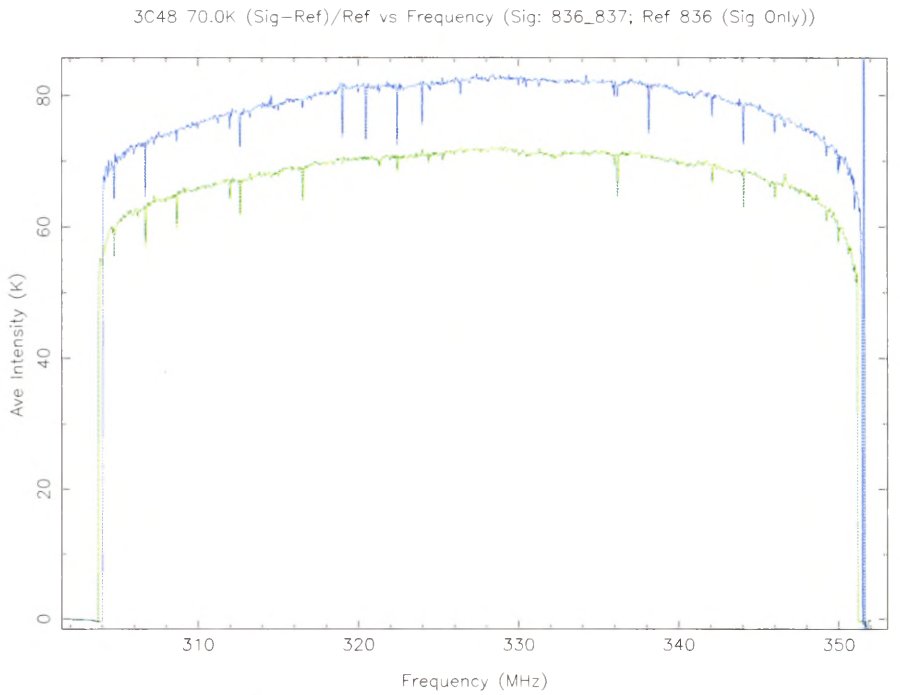

Figure 13: LCP and RCP spectra of 3C48 produced by $T_{sys} \times (Signal - Reference)/Reference$ calibration. This is the output of the `flare([836,837],836)` glish script.

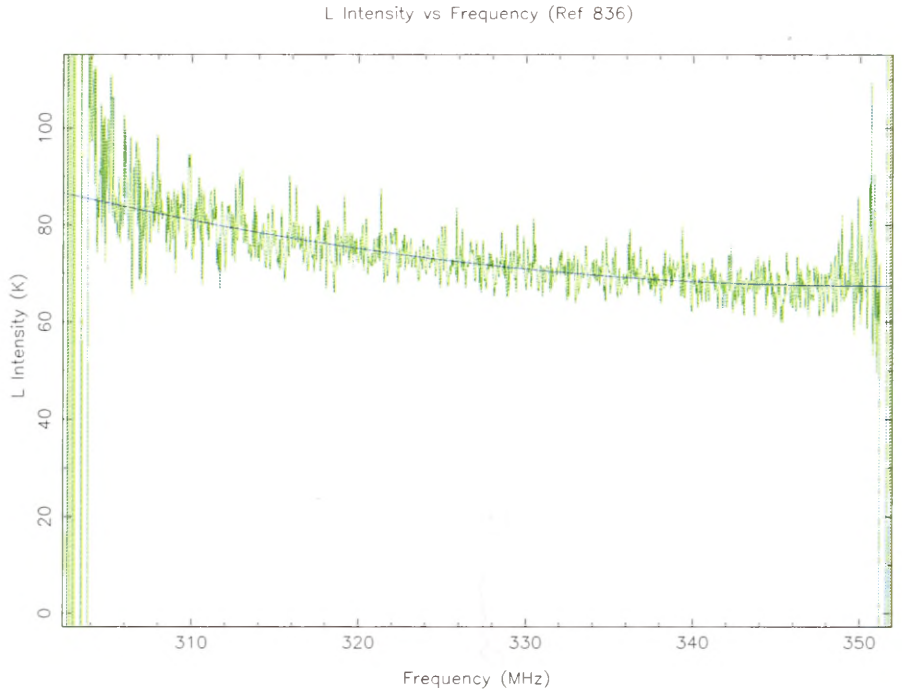

Figure 14: LCP spectrum measured for the system temperature of the reference scan. A second order polynomial was fit to the data.

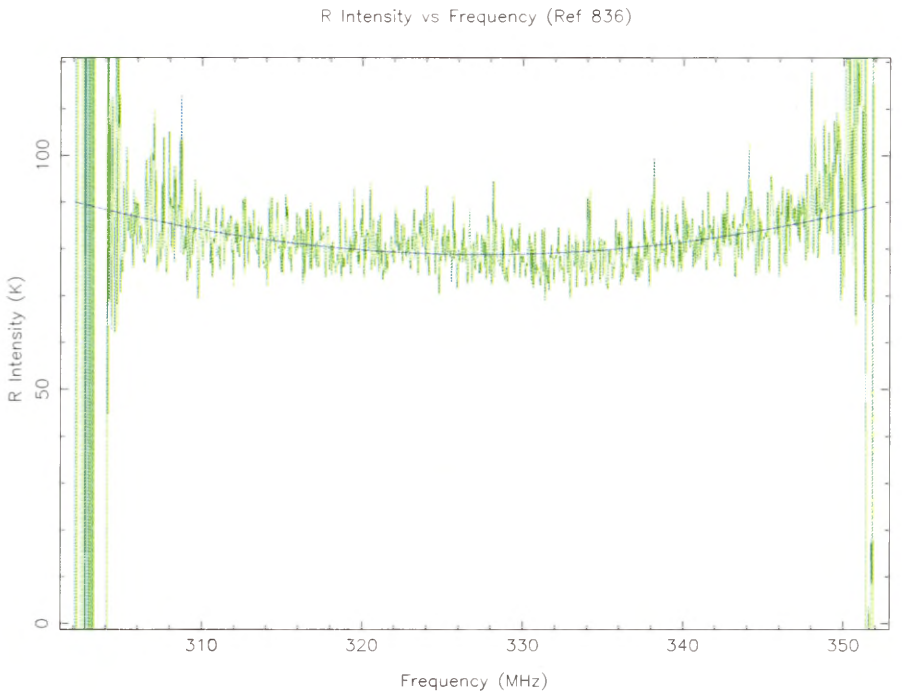

Figure 15: RCP spectrum measured for the system temperature of the reference scan. A second order polynomial was fit to the data.

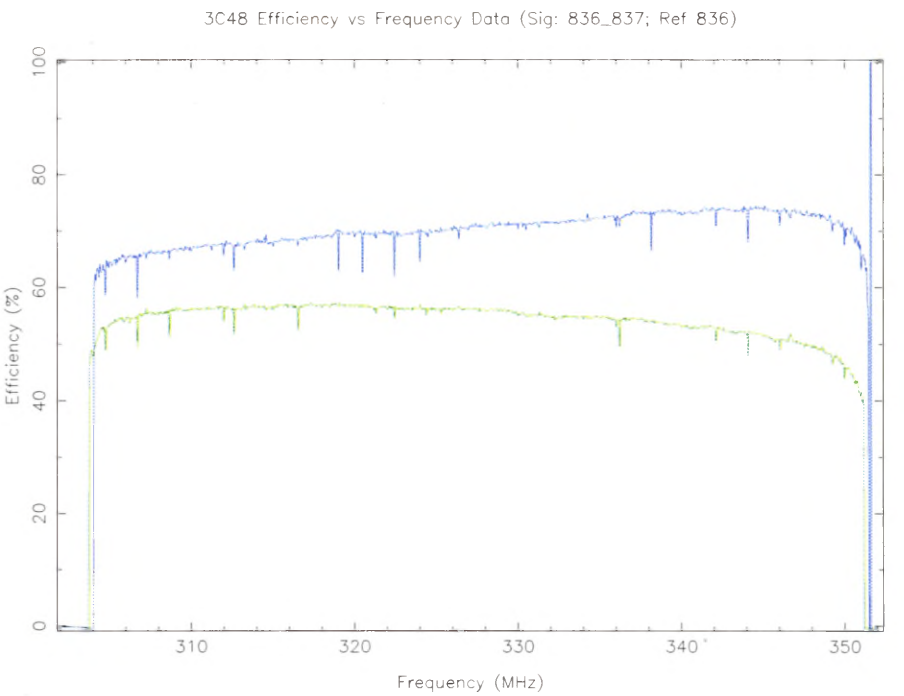

Figure 16: Measured GBT Efficiency based on observations of 3C48. This and the following plots are produced by glish scripts: `setFluxes(); updateEfficiency()`

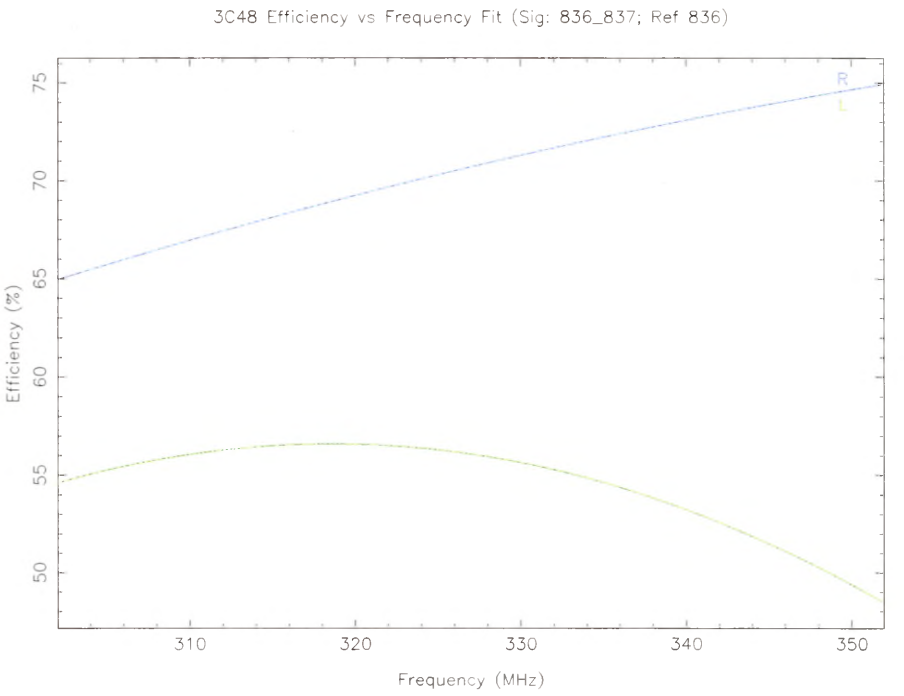

Figure 17: Fit to 3C48 LCP and RCP efficiency data, over the central 80% of the data in the previous plot.

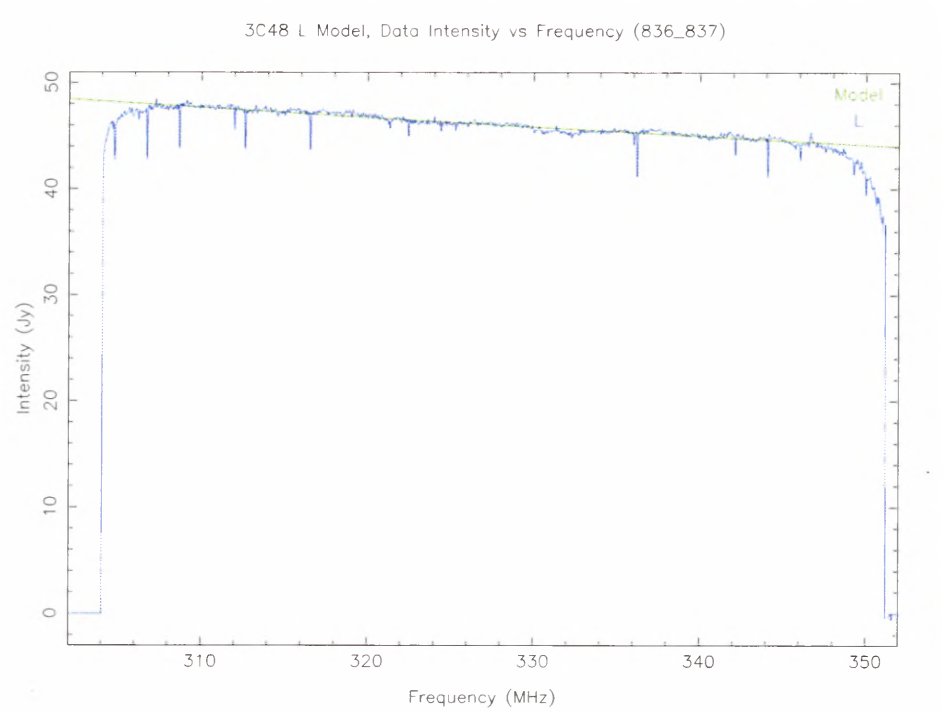

Figure 18: Spectral comparison of the calibrated 3C48 LCP observation with the Ott *et al.*1994 model for 3C48.

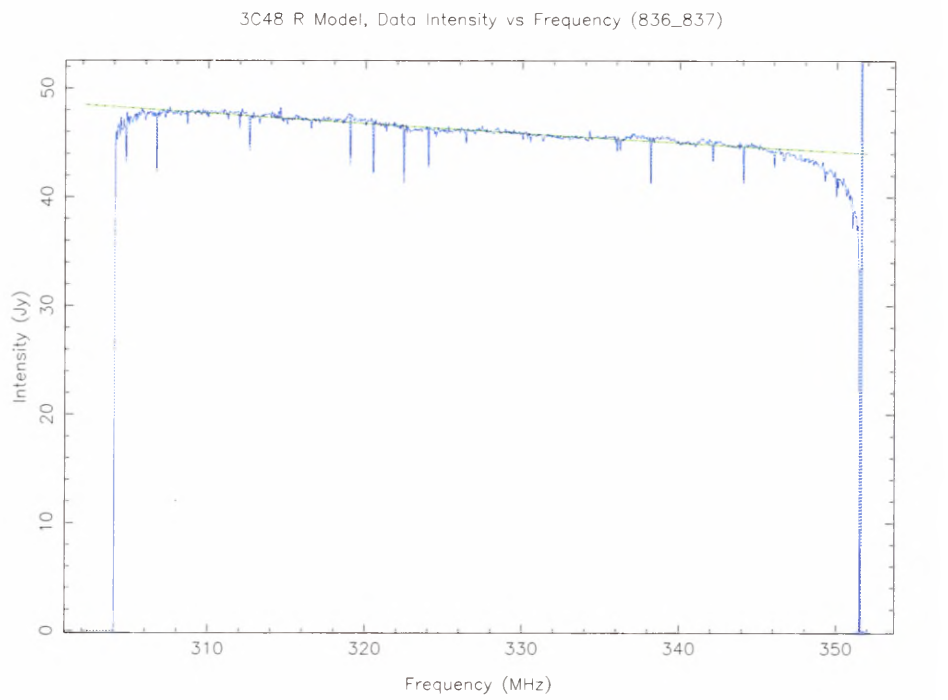

Figure 19: Spectral comparison of the calibrated 3C48 RCP observation with the Ott *et al.*1994 model for 3C48.

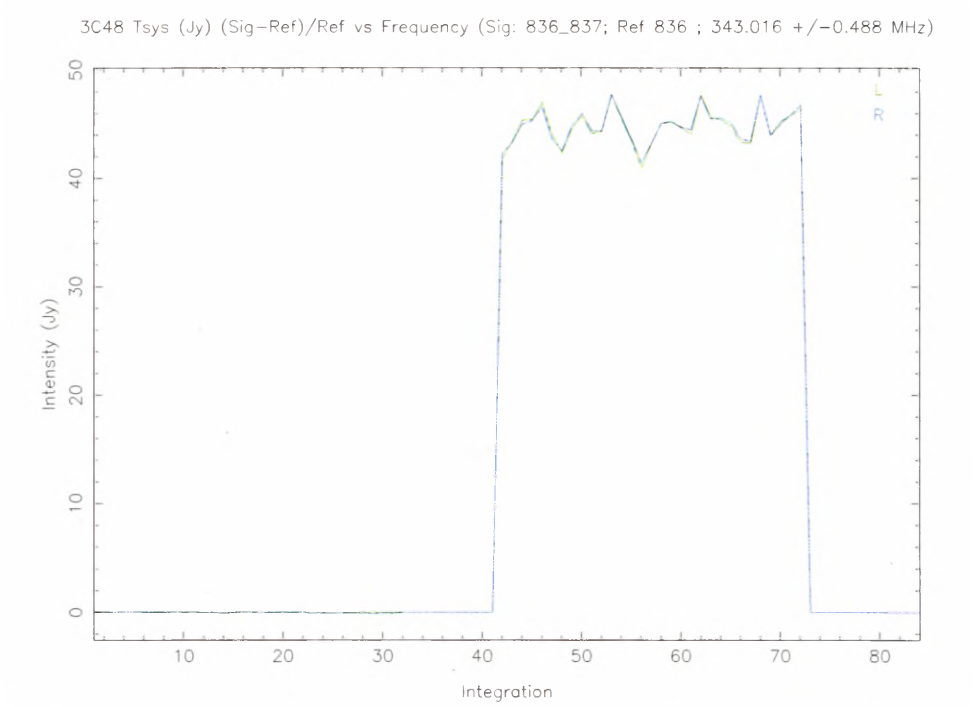

Figure 20: Average intensity versus time plot for the frequency range 342.5 to 343.5 MHz for reference and signal scans towards 3C48. The data are $T_{sys} \times (Sig - Ref)/Ref$ calibrated separately for LCP and RCP data. The average reference spectra for this time range was subtracted from both reference and signal. There are 10 integrations with zero intensity after each scan.

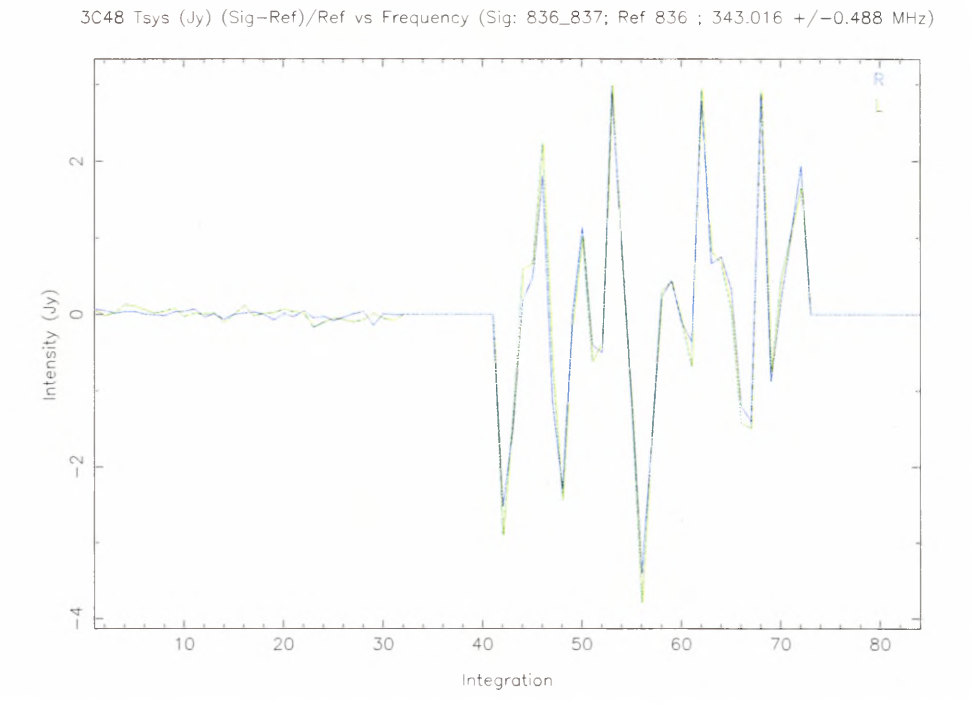

Figure 21: Average intensity versus time plot for the frequency range 342.5 to 343.5 MHz for reference and signal scans towards 3C48. The plot is the same as the previous plot, except that the average 3C48 intensity is subtracted from the signal scan. This shows the increased intensity variations toward 3C48.